Pyrene Schiff Base: Photophysics, Aggregation Induced Emission, and Antimicrobial Properties

ARTICLE *in* THE JOURNAL OF PHYSICAL CHEMISTRY B · OCTOBER 2014

Impact Factor: 3.3 · DOI: 10.1021/jp509697n

THE JOURNAL OF PHYSICAL CHEMISTRY B

Article

pubs.acs.org/JPCB

Pyrene Schiff Base: Photophysics, Aggregation Induced Emission, and Antimicrobial Properties

Arunkumar Kathiravan,*[,†] Karuppasamy Sundaravel,[‡] Madhavan Jaccob,[§] Ganesan Dhinagaran,[†] Angappan Rameshkumar,[∥] Devanesan Arul Ananth,[⊥] and Thilagar Sivasudha[⊥]

[†]National Centre for Ultrafast Processes, University of Madras, Taramani Campus, Chennai 600 113, Tamil Nadu, India

[‡]Chemical Laboratory, CSIR-Central Leather Research Institute, Adyar, Chennai 600 020, Tamil Nadu, India

[§]Department of Chemistry, Loyola College, Chennai 600 034, Tamil Nadu, India

[∥]TUV-SUD, PS - Chemical Lab, Bangalore 560 058, Karnataka, India

[⊥]Department of Environmental Biotechnology, Bharathidasan University, Tiruchirappalli 620 024, Tamil Nadu, India

Supporting Information

ABSTRACT: Pyrene containing Schiff base molecule, namely 4-[(pyren-1-ylmethylene)amino]phenol (KB-1), was successfully synthesized and well characterized by using ^{1}H, ^{13}C NMR, FT-IR, and EI-MS spectrometry. UV−visible absorption, steady-state fluorescence, time-resolved fluorescence, and transient absorption spectroscopic techniques have been employed to elucidate the photophysical processes of KB-1. It has been demonstrated that the absorption characteristics of KB-1 have been bathochromatically tuned to the visible region by extending the π-conjugation. The extended π-conjugation is evidently confirmed by DFT calculations and reveals that $\pi \rightarrow \pi^*$ transition is the major factor responsible for electronic absorption of KB-1. The photophysical property of KB-1 was carefully examined in different organic solvents at different concentrations and the results show that the fluorescence of this molecule is completely quenched due to photoinduced electron transfer. Intriguingly, the fluorescence intensity of KB-1 increases enormously by the gradual addition of water up to 90% with concomitant increase in fluorescence lifetime. This clearly signifies that this molecule has aggregation-induced emission (AIE) property. The mechanism of AIE of this molecule is suppression of photoinduced electron transfer (PET) due to hydrogen bonding interaction of imine donor with water. A direct evidence of PET process has been presented by using nanosecond transient absorption measurements. Further, KB-1 was successfully used for antimicrobial and bioimaging studies. The antimicrobial studies were carried out through disc diffusion method. KB-1 is used against both Gram-positive (*Rhodococcus rhodochrous* and *Staphylococcus aureus*) and Gram-negative (*Escherichia coli* and *Pseudomonas aeruginosa*) bacterial species and also fungal species (*Candida albicans*). The result shows KB-1 can act as an excellent antimicrobial agent and as a photolabeling agent. *S. aureus*, *P. aeruginosa*, and *C. albicans* were found to be the most susceptible microorganisms at 1 mM concentration among the bacteria used in the present investigation.

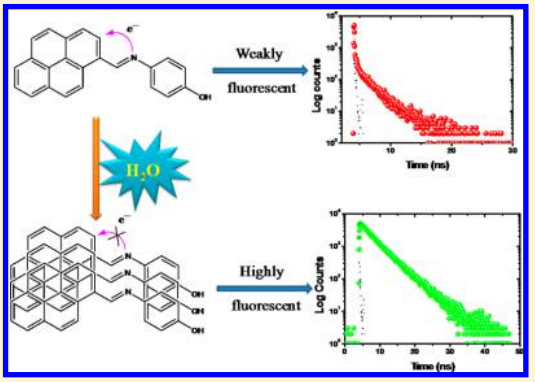

INTRODUCTION

In recent years, appropriate design and synthesis of efficient, stable, organic fluorescent materials has been a subject of interest in the area of organic light-emitting diodes (OLEDs).[1,2] OLED materials possess a potential for application in next-generation flat panel displays and solid-state lighting.[3−5] Other than use in OLEDs, these materials also find promising application in the field of sensors, bioimaging, solar cells, and lasers. However, the light emission of chromophores is usually quenched via aggregation, which is commonly known as aggregation-caused quenching (ACQ) effect.[6] This is a remarkable issue in the emerging area of developing a new material with fluorescence sensing systems. The ACQ effect is also a major obstacle in the fabrication of efficient OLEDs where the luminophores are used as a thin solid film. In the solid state, ACQ effect will be predominant if the luminophore concentration reaches its maximum owing to the absence of solvent. Birks[7] demonstrated that the ACQ effect is common to most of the aromatic hydrocarbons and their derivatives since these possess planar π-conjugated aromatic rings. So this may increase the possibility of $\pi-\pi$ stacking leading to the formation of excimers and exciplexes. It is then necessary to develop new luminophoric materials which can aggregate that emit more efficiently than monomers in solution. This is associated with two unusual phenomena exactly opposite the ACQ that have been identified by Tang et al.[8−12] One is the aggregation-

Received: September 26, 2014
Revised: October 30, 2014

   dx.doi.org/10.1021/jp509697n | J. Phys. Chem. B XXXX, XXX, XXX−XXX

induced emission enhancement (AIEE), which is largely due to the light emission of a chromophoric material enhanced by aggregate formation. The other one is the nonemissive material which is induced to emit by aggregation, which is known as aggregation-induced emission (AIE).

In 2001, Tang and co-workers reported the first AIE active compounds based on the pentaphenyl derivatives of silole and showing a weak fluorescent nature in solution but exhibiting intense fluorescence after aggregation.[8] The fluorescence quantum yields of siloles in aggregates is found to be a few hundred times higher than those quantum yields in solutions. They also reported that the mechanism of AIE is associated with the restriction of intramolecular rotation (RIR) of chromophoric compound. In continuation of this, numerous reports have appeared on AIE active dyes, which include siloles,[13] tetraphenylethane (TPE),[14] 9,10-bis(*p*-dimethylaminostyryl)-anthracene (9,10-MADSA),[15] 1-cyano-*trans*-1,2-bis-(40-methyl biphenyl)ethylene (CN-MBE),[16] 2,5-diphenyl-1,4-distyryl-benzene (DPDSB) derivatives,[17] diphenyldibenzofulvene (DPDBF) derivatives,[18] conjugated polymers,[19] borondipyrromethene (BODIPY) derivatives,[20] triazoles,[21] and others.[22,23] Several mechanisms has been postulated which involve the J-aggregation (head to tail), restriction of intramolecular charge transfer (ICT), twisted intramolecular charge transfer (TICT), and *cis*−*trans* isomerization. Among the various materials, pyrene is a classical example of a highly conjugated aromatic chromophore that emits deep blue light with high quantum efficiency in dilute solution, but which aggregates in the condensed state.[24,25] Indeed, the long fluorescence lifetime, high charge carrier mobility, and chemical stability make it a potentially good candidate for OLED applications. Chan et al. demonstrated an efficient blue-light-emitting diode based on solution processable pyrene-1,3-*alt*-calix[4]arene[26] with a record current efficiency of 10.5 cd A^{-1}.

Schiff bases are some of the most widely used organic compounds. They are used as pigments and dyes, catalysts, intermediates in organic synthesis, and polymer stabilizers. Schiff bases have also been shown to exhibit a broad range of pharmacological activities such as antifungal, antibacterial, antimalarial, antitubercular, antiproliferative, anti-inflammatory, antiviral, and antipyretic properties. Imine or azomethine groups are present in various natural, natural-derived, and non-natural compounds. The imine group present in such compounds has been shown to be critical to their biological activities,[27−29] which can be altered depending upon the type of substituent present on the aromatic rings. In view of these above biological properties of Schiff bases, we plan to synthesize pyrene-based Schiff base by Schiff condensation reaction. Recently, Wang et al. reported that phenylbenzoxazole-containing Schiff bases exhibit the aggregation-induced enhanced emission (AIEE) behavior in THF−water.[30] Recently, Jiang et al. showed that phenolic Schiff base bearing a pyrene group has the ability for use as a single molecular anion sensor.[31] Also, the derivative of 1-aminopyrene was used as a fluorescent chemodosimeter for the selective detection of Nb^{5+} ions in solution.[32] In all of the above articles, there was no focus on the mechanism of the fluorescence quenching. It is very important to study and rationalize the AIE aspects of the pyrene derivatives, through which one can be able to understand the quenching mechanism and develop the potential applications of pyrene derivatives in various emerging fields.

With suitable analysis, we planned to investigate the AIE properties of pyrene Schiff base (Scheme 1) and attempted to clarify the origins for light emission and causes of the AIE process. DFT calculations are also performed to study the electronic structure and photophysical properties of KB-1. Another interesting part of the present work is to probe the antimicrobial properties of pyrene Schiff base. The abbreviation of KB-1 is being used as alternative of 4-((pyren-1-ylmethylene)-amino)-phenol, a pyrene Schiff base.

Scheme 1. Structure of 4-((Pyren-1-ylmethylene)-amino)-phenol

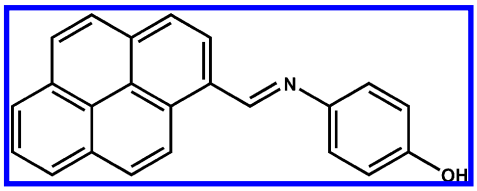

MATERIALS AND METHODS

Pyrene-1-carboxaldehyde and 4-aminophenol were purchased from Sigma-Aldrich chemicals. Synthetic grade solvents such as methanol were purchased from SRL. Spectroscopic grade solvents such as *N*,*N*′-dimethylformamide (DMF) and tetrahydrofuran (THF) were used for the spectral and electrochemical analysis. All measurements were performed at ambient temperature, except for laser flash photolysis studies.

Electronic absorption spectra of the samples were recorded using an Agilent 8453 UV−visible diode array spectrophotometer. The fluorescence spectral measurements were carried out using a Fluoromax-4 spectrophotometer (Horiba Jobin Yvon). For fluorescence studies, dilute solutions were used to avoid spectral distortions due to the inner-filter effect and emission reabsorption. Transient absorption experiments were carried out using nanosecond laser flash photolysis (Applied Photophysics, UK). The second harmonic (355 nm) of a Q-switched Nd:YAG laser (Quanta-Ray, LAB 150, Spectra Physics, USA) with 8-ns pulse width and 150-mJ pulse energy was used to excite the samples. The transients were probed using a 150-W pulsed xenon lamp, a Czerny−Turner monochromator, and a Hamamatsu R-928 photomultiplier tube as detector. The transient signals were captured with an Agilent Infiniium digital storage oscilloscope, and the data were transferred to the computer for further analysis. For laser flash photolysis studies, samples were purged with argon gas for about 45 min prior to the laser irradiation. Time-resolved fluorescence decays were obtained by the time-correlated single-photon counting (TCSPC) technique exciting the sample at 400 nm. Data analysis was carried out by the software provided by IBH (DAS-6), which is based on deconvolution techniques using nonlinear least-squares method, and the quality of the fit is ascertained with the value of χ^2 < 1.2.

FT-IR spectrum of KB-1 was recorded on a Bruker Vertex 70 (ATR-FTIR) spectrometer. NMR spectra were obtained on a Bruker spectrometer operating at 400 MHz for ^{1}H and 100 MHz for ^{13}C and collected at ambient probe temperature using DMSO as solvent unless otherwise mentioned. Chemical shifts are reported in δ (ppm) relative to TMS (^{1}H) or DMSO (^{13}C) as internal standards. Integrals are in accordance with assignments; coupling constants are given in Hz. All ^{13}C

dx.doi.org/10.1021/jp509697n | J. Phys. Chem. B XXXX, XXX, XXX−XXX

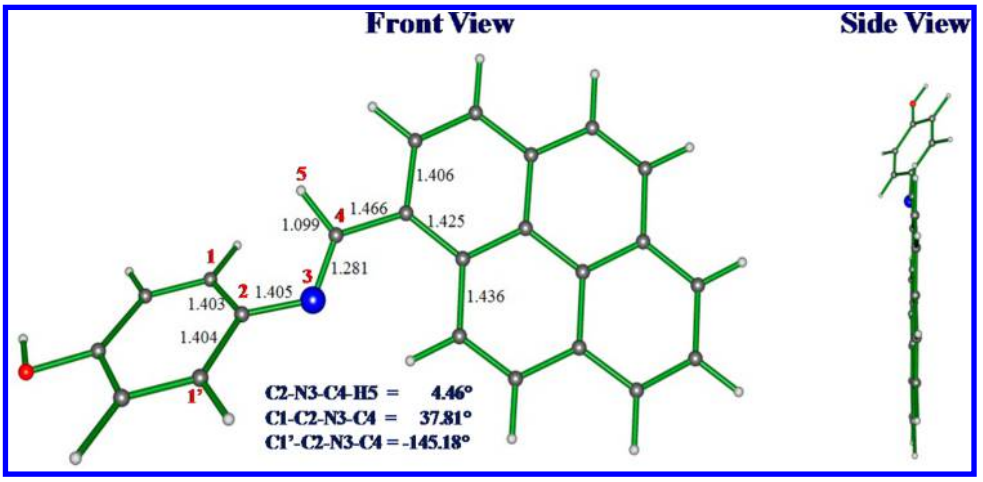

Figure 1. Optimized structure of KB-1.

spectra are proton-decoupled. EI-MS analyses were recorded using a JEOL GC Mate-II mass spectrometer PMT detector.

Fluorescence quantum yield (ϕ_F) for KB-1 was calculated in THF with quinine sulfate as the reference (ϕ_R = 0.53)[33] by using eq 1

$$\phi_F = (A_R/A_S)(I_S/I_R)(\eta_S/\eta_R)^2\phi_R \quad (1)$$

where the subscript S refers to the samples, the subscript R refers to quinine sulfate, A is the absorbance at the excitation wavelength, I is the integrated emission area, and η is the solvent refraction index.

All the computational calculations were performed using the Gaussian 09 suite.[34] Ground-state geometry optimization of KB-1 was carried out with hybrid exchange-correlation B3LYP functional in combination with 6-311+g(d,p) basis set.[35−37] Stationary points were located and characterized through computing the vibrational frequencies of KB-1. Vertical excitation energy, absorption wavelength, and oscillator strength on the ground-state optimized geometries were calculated using time-dependent density functional theory (TDDFT)[38] at B3LYP level using 6-311++g(d,p) basis set. The self-consistent reaction field−polarizable continuum model (SCRF-PCM)[39] was used to examine the THF solvent effect on the calculated properties of the species.

RESULTS AND DISCUSSION

The KB-1 molecule was synthesized according to the synthetic routes shown in Scheme S1 in the Supporting Information (SI). The synthetic route and structure characterization data are provided in SI Figures S1−S4.

Theoretical Consideration on Electronic Structure of KB-1. To understand the electronic structure of KB-1, we have employed density functional theory (DFT) calculations. DFT optimized geometries of KB-1 (Figure 1) clearly reveal that phenol group of KB-1 is found to be deviated from the plane of the 4-((pyren-1-ylmethylene)amino) group plane with an angle of −145.18°. So, the phenol substituted derivative of 4-((pyren-1-ylmethylene)amino) is found to have a less planar structure. This is clearly understandable from the side view of the optimized geometry of KB-1. The less planar structure of KB-1 could be due to the steric repulsions between the hydrogen atoms of the phenyl ring and the hydrogen atoms of C4. The computed absorption spectrum of KB-1 (SI Figure S5) displays a strong band at 441 nm with low excitation energy of 2.81 eV which is deviated from experimental absorption spectrum of KB-1 by 47 nm. It is known that B3LYP computed absorption wavelength is normally deviated from experimental absorption values on the order of 50 nm.[40] It is important to note that KB-1 shows $S_0 \rightarrow S_1$ electronic transition with large oscillator strength (f) of 0.82. $S_0 \rightarrow S_1$ transition mainly corresponds to the orbital transition from the highest occupied molecular orbital (HOMO) to the lowest occupied molecular orbital (LUMO). Detailed inspection of MOs in Figure 2 clearly shows

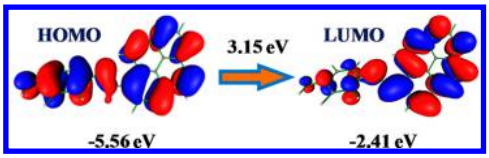

Figure 2. HOMO−LUMO energy levels of KB-1.

that the majority of electronic distribution of the HOMO and LUMO was found to be located on the entire KB-1 molecule. The intensity of the computed band at 441 nm largely derives from the HOMO−LUMO transition (93%) with a contribution from the π-bonding orbital of entire KB-1 to the respective π-antibonding orbital of KB-1. Thus, S_1 state of KB-1 shows the $\pi \rightarrow \pi^*$ character. From the calculated data, the HOMO−LUMO gap of KB-1 is found to be 3.15 eV, which is lower than that of the calculated HOMO−LUMO gap of pyrene group alone (3.80 eV). The decrease in the HOMO−LUMO gap of KB-1 with respect to the parent pyrene is due to the extended conjugation through imino-phenol group even though KB-1 has the less planar structure.

Photophysics in Solution. KB-1 is readily and copiously soluble in organic solvents such as acetone, THF, DMF, and DMSO, but it is insoluble in methanol, ethanol, acetonitrile, and water. So, we have recorded the UV−vis absorption spectra of KB-1 in DMF (ε_s = 36.7) and THF (ε_s = 7.58) with different dielectric constant. In both solvents, an intense absorption band is observed around 394 nm (Figure 3). With the help of DFT calculations, this absorption band can be attributed to the $\pi \rightarrow \pi^*$ transition resulting from the extended conjugation between the aromatic ring and nitrogen atom. In general, pyrene derivatives are very prone to aggregate in solution, and as a result peak shifting or broadening of absorption spectrum should be observed. Keeping in mind, to understand the aggregation behavior of KB-1, we have measured the absorption

dx.doi.org/10.1021/jp509697n | J. Phys. Chem. B XXXX, XXX, XXX−XXX

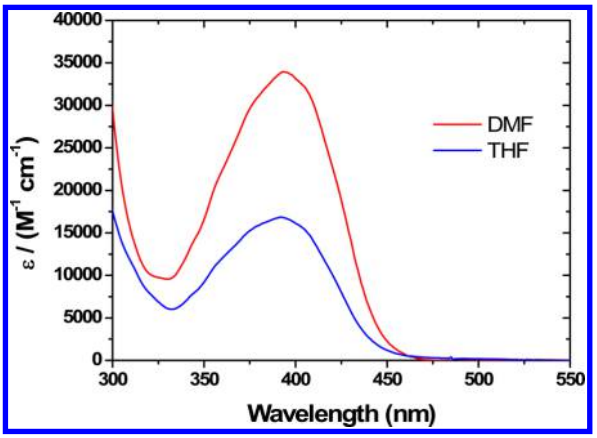

Figure 3. Absorption spectrum of KB-1 in DMF and THF solvents.

spectrum of KB-1 at different concentrations in DMF and THF solvents by using absorption spectroscopy. As can be seen from SI Figure S6, while increasing the concentration of KB-1, the intensity of absorbance increases and there are no new bands observed in either DMF or THF solvents. At the same time, Beer–Lambert law was also obeyed for KB-1 in the concentration ranges from 10 to 50 μM showing that the KB-1 is not significantly aggregated within this concentration range. It should be noted that the extinction coefficient value is higher for DMF (3.6×10^4 M^{-1} cm^{-1}) than THF (2.2×10^4 M^{-1} cm^{-1}).

To understand the excited state behavior of KB-1, we have measured the fluorescence spectrum of KB-1 (10 μM), exciting at 400 nm. Intriguingly, KB-1 exhibited very weak fluorescence in both solvents (Figure 4a). There are many possible reasons for a weak fluorescence in solution, such as concentration quenching, photoinduced electron transfer, and energy transfer, etc. We have recorded fluorescence spectrum of KB-1 by varying concentration in the range of 50 to 0.1 μM, however, we could not observe any fluorescence of KB-1; this clearly indicates that there is no concentration quenching effect existing in this system (spectrum not shown here). Another possible mechanism is energy transfer. For energy transfer, the excited state of donor should overlap with ground state of the acceptor. In the present case, there is no overlap between fluorescence of pyrene and absorption of *p*-aminophenol, indeed indicating that there is no energy transfer present in KB-1 molecule. So, the only possible mechanism existing in KB-1 molecule is photoinduced electron transfer (PET). To support our speculation, recently, Pradeep et al. reported that the very weak fluorescence of the pyrene-based Schiff base is mainly due to PET, which arises from the imine nitrogen to the photoexcited pyrene moiety.[32] Jiang et al. also reported a similar kind of PET mechanism from the imine nitrogen to the photoexcited pyrene moiety.[31] However, they did not explain the dynamics of PET process. In this context, we have employed both time-resolved absorption and fluorescence spectroscopic techniques to explain the PET process.

With the help of the time-resolved fluorescence technique, one can monitor the lifetime of a fluorophore and track the electron transfer process between dyad systems.[41] Based on this context, we have measured the excited-state decay curve of KB-1 using the time-correlated single-photon counting (TCSPC) technique to evaluate the PET process. Figure 4b demonstrates the excited-state decay of KB-1 collected in both DMF and THF solvents upon excitation at 400 nm, and the emission was

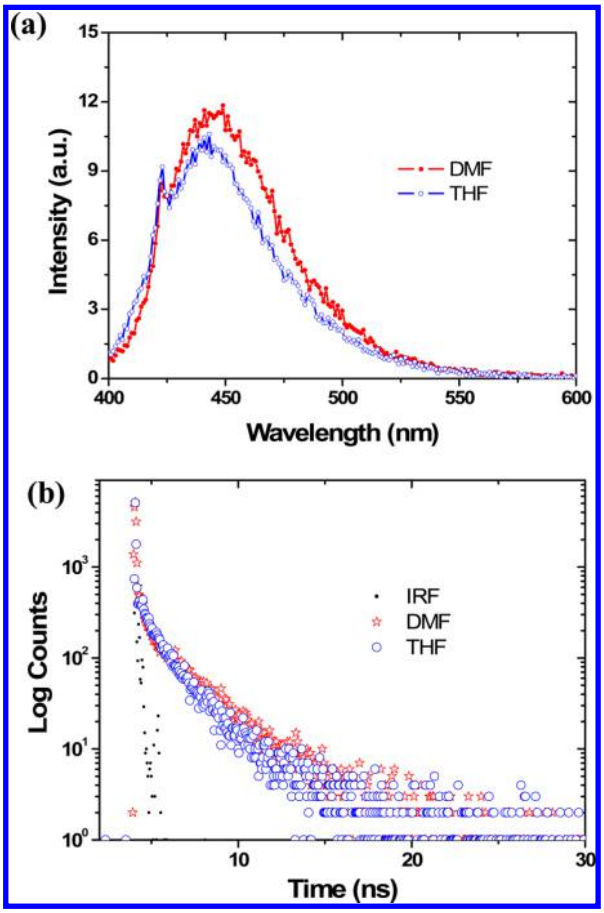

Figure 4. (a) Steady-state and (b) time-resolved fluorescence of KB-1 (10 μM) in DMF and THF solvents.

observed at 440 nm. In both solvents, KB-1 exhibits short- and long-lived decay, and the fitted decay parameters are listed in Table 1. From the data, it is clear that the shorter component is

Table 1. Fluorescence Lifetime Data of KB-1

solvent	τ_1 (ns)	A_1 (%)	τ_2 (ns)	A_2 (%)	k_{et} (10^9 s^{-1})
DMF	0.27	29	2.19	71	3.25
THF	0.44	23	1.69	77	1.61

attributed to the deactivation (quenching) of the excited pyrene moiety by imine group and the long-lived component is assigned to an unquenched decay of the KB-1. The observed shorter component is entirely due to electron transfer, therefore, the rate constant of electron transfer (k_{et}) can be calculated by using eq 2[42]

$$k_{et} = 1/\tau_S - 1/\tau_L \quad (2)$$

where τ_S is the short-lived component and τ_L is the long-lived component. The obtained k_{et} is depicted in Table 1; the values are on the order of 10^9 which clearly indicates that PET is efficient in this system.[43]

To gain a deeper understanding of the electron processes, KB-1 sample was subjected to transient absorption studies in deaerated THF. Upon excitation using 355 nm (Nd:YAG, third harmonic), the transient absorption spectrum of KB-1 (Figure 5) exhibited ground-state depletion at 340 nm and transient absorption maximum at 490 nm. It is well-known that the triplet state of organic molecules is generally efficiently

dx.doi.org/10.1021/jp509697n | J. Phys. Chem. B XXXX, XXX, XXX–XXX

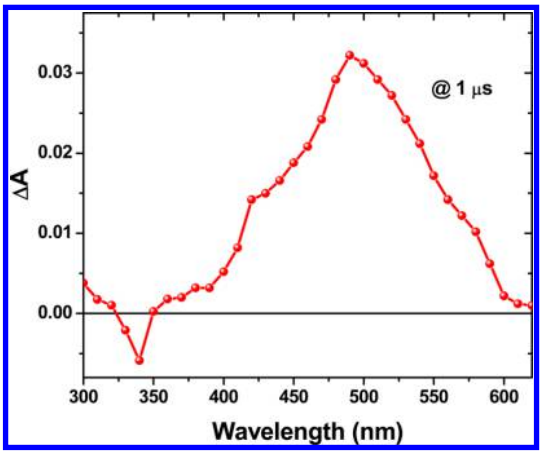

Figure 5. Transient absorption spectrum of KB-1 in THF.

quenched by oxygen. However, in the presence of oxygen (ambient atmosphere), the transient spectrum of KB-1 still remains the same, which suggest that the obtained transient is not due to triplet species. Therefore, we unambiguously assigned the transient of KB-1 to anion radical of pyrene due to photoinduced electron transfer. This is in accordance with the existing literature.[44] Ultrafast laser spectroscopy studies, to be published elsewhere, are presently being performed on these derivatives to determine the rate of electron injection and recombination dynamics.

Perhaps the most striking result of the photophysics is that complete fluorescence quenching of KB-1 is due to PET as evidenced by obtained short-lived fluorescence decay using time-resolved fluorescence technique. Moreover, the obtained pyrene radical anion using time-resolved absorption spectroscopy is incontrovertible proof of PET process.

Aggregation-Induced Emission (AIE) Properties. When a nonemissive molecule is induced to emit by aggregate formation, the molecule is referred to as an "AIE active" molecule. To explore whether KB-1 is AIE active or not, the UV–vis absorption spectrum of KB-1 (10 μM) was recorded in the presence of different percentages of water (Figure 6 and SI Table S1).

KB-1 shows the broad absorption peak in the range of 350–450 nm in THF. Upon addition of different amounts of water (SI Tables S1 and S2), KB-1 aggregates due to interaction with water as evident by splitting of single characteristic peak into two peaks. Similar results were also obtained in DMF; spectra are shown in SI Figure S7. Generally, blue shift in absorption results from H-type aggregation and red shift in absorption is due to J-type aggregation. However, in the present case blue shift absorption was observed upon increasing the percentage of water, which clearly discloses that H-type aggregates are formed (i.e., head–head interaction) and there is a noticeable color change observed from colorless to bluish color under the UV light illumination upon addition of 90% of water (Figure 7). This clearly indicates that KB-1 molecule is AIE active, and this phenomenon is verified by employing both steady-state and time-resolved fluorescence spectroscopy.

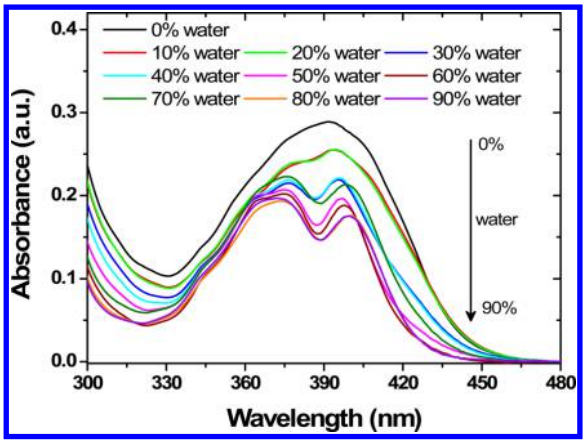

Figure 6. Absorption spectrum of KB-1 in THF with increasing percentage of water.

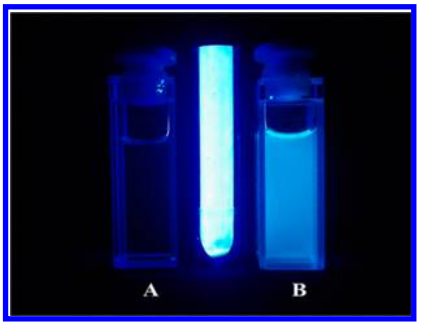

Figure 7. (A) KB-1 in THF and (B) KB-1 in THF/water mixture. Photographs taken under illumination of a UV lamp.

The fluorescence spectrum of KB-1 in THF and THF containing different amounts of water was recorded (Figure 8).

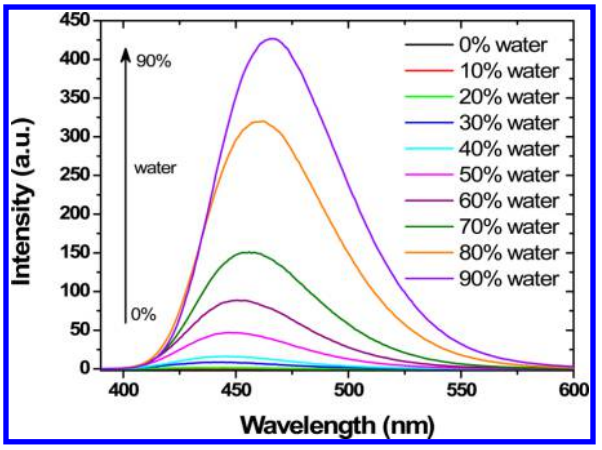

Figure 8. Emission spectrum of KB-1 in THF with increasing percentage of water.

From this figure, it can be seen that completely quenched emission is enhanced significantly when a large amount of water is added. Upon addition of water to the THF solution of KB-1, the emission intensity remains unchanged up to 70% of water. Successive addition of water enhances the emission intensity with a red shift (25 nm) from 440 to 465 nm, and reaching maximum at 90% of water. The proposed mechanism for the enhanced emission is due to suppression of PET due to hydrogen bonding interaction of imine donor with water. Because of hydrogen bonding interaction, the molecules aggregate and as a result KB-1 molecule is more emissive. The proposed mechanism is clearly visualized in the Abstract Graphic. A similar kind of emission behavior is also observed

dx.doi.org/10.1021/jp509697n | J. Phys. Chem. B XXXX, XXX, XXX–XXX

for other Schiff base systems,[30] revealing that those molecules are AIE active. Moreover, there is a noticeable change of color from colorless to bluish under the UV light after the addition of 90% of water (Figure 7). Thus, the above spectral results reveal that KB-1 possesses AIE property. To check what is special in THF/water mixtures, we have chosen DMF in the place of THF, which is also miscible in water. In the presence of water (90%), the emission was also intensified and red-shifted as observed in THF/water mixture (SI Figure S8). Most interesting is that the normalized emission of aggregates from both mixtures is nearly the same, suggesting that the formed aggregates are not affected by the surrounding of the solvent molecules (SI Figure S9a). Moreover, the plot of emission intensity against the percentage of water clearly demonstrates that THF/water mixture shows more intense emission than DMF/water mixture (SI Figure S9b). In addition to that. the observed quantum yield is higher for THF/water mixture (ϕ = 0.47) than that of DMF/water mixture (ϕ = 0.32). This is possibly due to KB-1 aggregating more in THF/water than DMF/water mixture as evident from absorption spectral studies.

Further, the AIE behavior of KB-1 in the excited state has been investigated by the TCSPC technique. By using this technique one can deduce the excited lifetime of the molecule, i.e. how long the molecule stays in the excited state. Moreover, measurement of fluorescence lifetime is more robust than measurement of fluorescence intensity, because it depends neither on the intensity of excitation nor on the concentration of the fluorophore. Figure 9 shows the fluorescence decay of

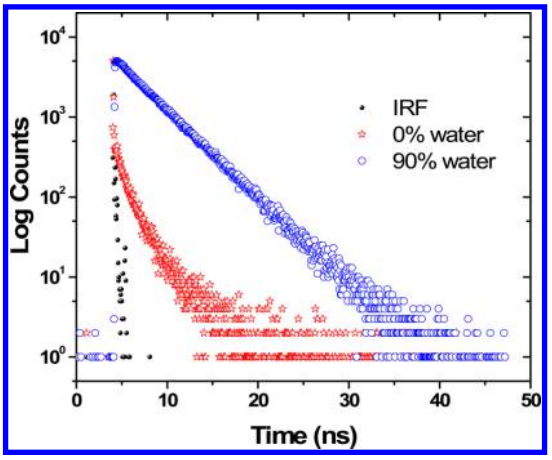

Figure 9. Fluorescence decay of KB-1 in THF and THF/water mixture.

KB-1 in THF and THF/water mixture. In the absence of water, KB-1 in THF exhibits biexponential decay with two distinct lifetimes of 1.69 ns (77%) and 0.44 ns (23%). After the addition of 90% H_2O, KB-1 shows single exponential decay with longer lifetime component (3.8 ns). The observed longer fluorescence lifetime is due to suppression of PET process caused by aggregation of the KB-1 molecules. It should be noted here that KB-1 in both mixtures (THF/water and DMF/water) furnishes identical fluorescence lifetimes, indicating that formed aggregates are not affected by the surrounding solvent molecules (SI Figure S10).

Antimicrobial Studies. Another intent of the present work is to verify the antimicrobial capability of KB-1 and further exploit it for antimicrobial applications through nanotechnology for drug delivery and photolabeling detection.[45] In recent decades, fluorescent compounds have found a wide range of applications in various biomedical fields.[46] In this paper, the newly prepared fluorescent compound KB-1 was examined for its antimicrobial activity and photolabeling studies. The antibacterial activity was tested against *E. coli*, *P. aeruginosa*, *R. rhodochrous*, *S. aureus*, and *C. albicans*.

The chemically synthesized compound KB-1 possesses antibacterial activity against Gram-positive and Gram-negative bacterial and fungal strains. KB-1 exhibited varying zones of inhibition (6−14 mm) for all the tested pathogens. But there is no zone formation against *E. coli*, *R. rhodochrous*, or *P. aeruginosa* at 0.5 mM concentration. Of all the tested organisms, *S. aureus*, *P. aeruginosa*, and *C. albicans* were found to be highly susceptible at 1 mM concentration among the microbial species tested in the present study. Gentamycin and Nystatin were used as standards against bacteria and fungi, respectively. Test results are shown in Figure 10 and the values are listed in Table 2. From the data, it is clear that KB-1 possesses high antibacterial activity against both Gram-positive and Gram-negative bacteria species. In addition, the antifungal

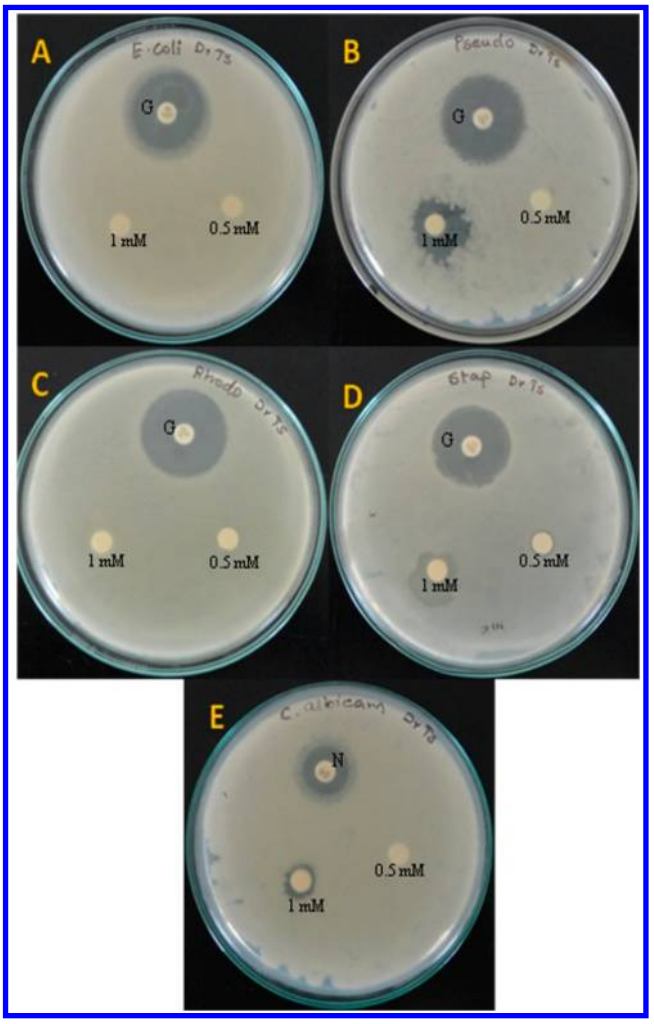

Figure 10. In vitro antimicrobial activity of KB-1 by disc diffusion method (A) *Escherichia coli*, (B) *Pseudomonas aeruginosa*, (C) *Rhodococcus rhodochrous*, (D) *Staphylococcus aureus*, and (E) *Candida albicans*.

dx.doi.org/10.1021/jp509697n | J. Phys. Chem. B XXXX, XXX, XXX−XXX

Table 2. In vitro Antibacterial Activity of KB-1[a]

	Gram positive bacteria		Gram negative bacteria		fungus
compound	*S. aureus* MTCC 96	*R. rhodochrous* MTCC 265	*E. coli* MTCC 739	*P. aeruginosa* MTCC 1934	*C. albicans* MTCC 227
KB-1 (1 mM)[b]	12	8	7	14	12
KB-1 (0.5 mM)[b]	7	NZ	NZ	NZ	6
Gentamycin[c]	22	28	30	24	
Nystatin[d]					20

[a]Zone of inhibition in mm, all results are expressed as triplicate. NZ: No zone formation. [b]30 μL/disc. [c]15 μg/disc. [d]10 μg/disc

result of *C. albicans* clearly indicates the antifungal capability of KB-1.

Further, the fluorescence property of KB-1 was analyzed by using fluorescence microscopy to probe the microbes (*P. aeruginosa* and *C. albicans*). Figure 11 shows the KB-1 treated

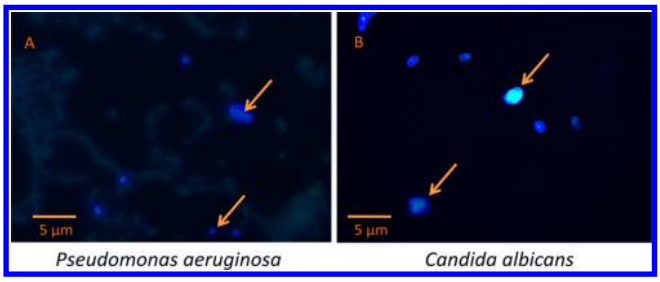

Figure 11. Fluorescent micrographs of (A) *Pseudomonas aeruginosa* and (B) *Candida albicans*. Arrow indicates the fluorescence of KB-1 treated microbes.

microbes (*P. aeruginosa* and *C. albicans*) with blue filter. The photolabeling of microbes using fluorophores was due to the interaction between hydrogen of KB-1 and amino acids from microbial cell wall.[47]

Generally, antimicrobial activity of chemically synthesized compounds follows stress-induced cell death, as antibiotics induce bacterial death through the activation of stress responses.[48] This may depend on the specific binding site of synthesized compound and cell wall receptors. The same basic mechanism might be involved in our study too; i.e., OH group in the active site of KB-1 might interact with cell wall or cell membrane proteins. Once the compounds adhere to the cell membrane, it will interact with membrane proteins and other microbial micro and macro molecules, finally increasing the cell membrane permeability. The permeability of microbial membrane will allow the intra cellular components to leak and result in lose of electrolytes such as Na^+, K^+, and Ca^{2+}, finally leading to cell death.[45,49] These results strongly suggest that KB-1 found to be the most effective antimicrobial agent as well as can act as photolabeling agent. Further studies are needed to comprehend the KB-1 induced antimicrobial mechanistic pathway against both bacteria and fungal species.

SUMMARY

We have investigated aggregation-induced emission and antimicrobial properties of a pyrene Schiff base. This molecule is found to be weakly fluorescent in THF solution; interestingly, the fluorescence intensity and fluorescence lifetime increased enormously by the gradual addition of water up to 90%. Time-resolved fluorescence measurements on KB-1 molecule were performed at different solvents to better understand the origin of aggregation-induced emission (AIE). The mechanism of AIE of this molecule is suppression of PET due to hydrogen bonding interaction of imine donor with water. With laser flash photolysis technique, direct evidence for the process of PET was obtained. Moreover, the obtained pyrene radical anion at 490 nm is an incontrovertible proof of PET process. In addition, KB-1 was successfully used for antimicrobial and bioimaging studies. Results showed that KB-1 was found to be a most effective antimicrobial agent as well as able to act as photolabeling agent. Further, in order to rationalize the electronic origin and mechanism of AIE properties of KB-1, detailed theoretical calculations are presently undergoing in our laboratory with other pyrene Schiff base derivatives.

ASSOCIATED CONTENT

Supporting Information

Synthesis, characterization, spectra, and additional figures as noted in the text. This material is available free of charge via the Internet at http://pubs.acs.org.

AUTHOR INFORMATION

Corresponding Author

*E-mail: akathir23@hotmail.com.

Notes

The authors declare no competing financial interest.

ACKNOWLEDGMENTS

A.K., K.S., and M.J. thank the Department of Science and Technology, India for DST-INSPIRE Faculty Award.

REFERENCES

(1) Chen, C. T. Evolution of Red Organic Light-Emitting Diodes: Materials and Devices. *Chem. Mater.* **2004**, *16*, 4389−4400.

(2) Yuan, W. Z.; Gong, Y.; Chen, S.; Shen, X. Y.; Lam, J. W. Y.; Lu, P.; Lu, Y.; Wang, Z.; Hu, R.; Xie, N.; et al. Efficient Solid Emitters with Aggregation-Induced Emission and Intramolecular Charge Transfer Characteristics: Molecular Design, Synthesis, Photophysical Behaviors, and OLED Application. *Chem. Mater.* **2012**, *24*, 1518−1528.

(3) Reineke, S.; Lindner, F.; Schwartz, G.; Seidler, N.; Walzer, K.; Lussem, B.; Leo, K. White Organic Light-Emitting Diodes with Fluorescent Tube Efficiency. *Nature* **2009**, *459*, 234−238.

(4) Sun, Y.; Giebink, N. C.; Kanno, H.; Ma, B.; Thompson, M. E.; Forrest, S. R. Management of Singlet and Triplet Excitons for Efficient White Organic Light-Emitting Devices. *Nature* **2006**, *440*, 908−912.

(5) Tonzani, S. Lighting Technology: Time to Change the Bulb. *Nature* **2009**, *459*, 312−314.

(6) Jenekhe, S. A.; Osaheni, J. A. Excimers and Exciplexes of Conjugated Polymers. *Science* **1994**, *265*, 765−768.

(7) Birks, J. B. *Photophysics of Aromatic Molecules*; Wiley: London, 1970.

(8) Luo, J.; Xie, Z.; Lam, J. W. Y.; Cheng, L.; Chen, H.; Qiu, C.; Kwok, H. S.; Zhan, X.; Liu, Y.; Zhu, D.; et al. Aggregation Induced Emission of 1-methyl-1,2,3,4,5-pentaphenylsilole. *Chem. Commun.* **2001**, 1740−1741.

(9) Zeng, Q.; Li, Z.; Dong, Y.; Di, C.; Qin, A.; Hong, Y.; Ji, L.; Zhu, Z.; Jim, C. K. W.; Yu, G.; et al. Fluorescence Enhancements of Benzene-Cored Luminophores by Restricted Intramolecular Rotations: AIE and AIEE Effects. *Chem. Commun.* **2007**, 70−72.
(10) Hong, Y.; Lam, J. W. Y.; Tang, B. Z. Aggregation Induced Emission. *Chem. Soc. Rev.* **2011**, *40*, 5361−5388.
(11) Zhao, Z.; Chen, S.; Chan, C. Y. K.; Lam, J. W. Y.; Jim, C. K. W.; Lu, P.; Chang, Z.; Kwok, H. S.; Qiu, H.; B.Z. Tang, B. Z. A Facile and Versatile Approach to Efficient Luminescent Materials for Applications in Organic Light-Emitting Diodes. *Chem.−Asian J.* **2012**, *7*, 484−488.
(12) Leung, C. W. T.; Hong, Y.; Chen, S.; Zhao, E.; Lam, J. W. Y.; Tang, B. Z. A Photostable AIE Luminogen for Specific Mitochondrial Imaging and Tracking. *J. Am. Chem. Soc.* **2013**, *135*, 62−65.
(13) Chen, J.; Law, C. C. W.; Lam, J. W. Y.; Dong, Y.; Lo, S. M. F.; Williams, I. D.; Zhu, D.; Tang, B. Z. Synthesis, Light Emission, Nanoaggregation, and Restricted Intramolecular Rotation of 1,1-Substituted 2,3,4,5-Tetraphenylsiloles. *Chem. Mater.* **2003**, *15*, 1535−1546.
(14) Shi, H.; Kwok, R. T. K.; Liu, J.; Xing, B.; Tang, B. Z.; Liu, B. Real-Time Monitoring of Cell Apoptosis and Drug Screening Using Fluorescent Light-Up Probe with Aggregation-Induced Emission Characteristics. *J. Am. Chem. Soc.* **2012**, *134*, 17972−17981.
(15) Wang, Y.; Liu, T.; Bu, L.; Li, J.; Yang, C.; Li, X.; Tao, Y.; Yang, W. Aqueous Nanoaggregation-Enhanced One and Two-Photon Fluorescence, Crystalline J-Aggregation-Induced Red Shift, and Amplified Spontaneous Emission of 9,10-Bis(*p*-dimethylaminostyryl)-anthracene. *J. Phys. Chem. C* **2012**, *116*, 15576−15583.
(16) An, B. K.; Kwon, S. K.; Jung, S. D.; S.Y. Park, S. Y. Enhanced Emission and Its Switching in Fluorescent Organic Nanoparticles. *J. Am. Chem. Soc.* **2002**, *124*, 14410−14415.
(17) Li, Y.; Li, F.; Zhang, H.; Xie, Z.; Xie, W.; Xu, H.; Li, B.; Shen, F.; Ye, L.; Hanif, M.; et al. Tight Intermolecular Packing Through Supramolecular Interactions in Crystals of Cyano substituted oligo-(*para*-phenylene vinylene): A Key Factor for Aggregation-Induced Emission. *Chem. Commun.* **2007**, 231−233.
(18) Dong, Y.; Lam, J. W. Y.; Qin, A.; Li, Z.; Sun, J.; Sung, H. H. Y.; Williams, I. D.; Tang, B. Z. Switching the Light Emission of (4-biphenylyl)phenyldibenzofulvene by Morphological Modulation: Crystallization-Induced Emission Enhancement. *Chem. Commun.* **2007**, 40−42.
(19) Deans, R.; Kim, J.; Machacek, M. R.; Swager, T. M. A Poly(*p*-phenyleneethynylene) with a Highly Emissive Aggregated Phase. *J. Am. Chem. Soc.* **2000**, *122*, 8565−8566.
(20) Perumal, K.; Garg, J. A.; Blacque, O.; Saiganesh, R.; Kabilan, S.; Balasubramanian, K. K.; Venkatesan, K. β-Iminoenamine-BF_2 Complexes: Aggregation-Induced Emission and Pronounced Effects of Aliphatic Rings on Radiationless Deactivation. *Chem.−Asian J.* **2012**, *7*, 2670−2677.
(21) Wang, J.; Mei, J.; Hu, R.; Sun, J. Z.; Qin, A.; Tang, B. Z. Click Synthesis, Aggregation-Induced Emission, *E*/*Z* Isomerization, Self-Organization, and Multiple Chromisms of Pure Stereoisomers of a Tetraphenylethene-Cored Luminogen. *J. Am. Chem. Soc.* **2012**, *134*, 9956−9966.
(22) Shustova, N. B.; McCarthy, B. D.; Dinca, M. Turn-On Fluorescence in Tetraphenylethylene-Based Metal−Organic Frameworks: An Alternative to Aggregation-Induced Emission. *J. Am. Chem. Soc.* **2011**, *133*, 20126−20129.
(23) Manimaran, B.; Thanasekaran, P.; Rajendran, T.; Lin, R. J.; Chang, I. J.; Lee, G. H.; Peng, S. M.; Rajagopal, S.; Lu, K. L. Luminescence Enhancement Induced by Aggregation of Alkoxy-Bridged Rhenium(I) Molecular Rectangles. *Inorg. Chem.* **2002**, *41*, 5323−5325.
(24) Reynders, P.; Kuhnle, W.; Zachariasse, K. A. Ground-State Dimers in Excimer-Forming Bichromophoric Molecules. 1. Bis-(pyrenylcarboxy)alkanes. *J. Am. Chem. Soc.* **1990**, *112*, 3929−3939.
(25) Zachariasse, K. A.; Macanita, A.; Kuhnle, W. Chain Length Dependence of Intramolecular Excimer Formation with 1,*n*-Bis(1-pyrenylcarboxy)alkanes for n = 1−16, 22, and 32. *J. Phys. Chem. B* **1999**, *103*, 9356−9365.
(26) Chan, K. L.; Lim, J. P. F.; Yang, X.; Dodabalapur, A.; Jabbour, G. E.; Sellinger, A. High-Efficiency Pyrene-based Blue Light Emitting Diodes: Aggregation Suppression using a Calixarene 3D-scaffold. *Chem. Commun.* **2012**, *48*, 5106−5108.
(27) O'Donnell, M. J. The Enantioselective Synthesis of α-Amino Acids by Phase-Transfer Catalysis with Achiral Schiff Base Esters. *Acc. Chem. Res.* **2004**, *37*, 506−517.
(28) Przybylski, P.; Huczynski, A.; Pyta, K.; Brzezinski, B.; Bartl, F. *Curr. Org. Chem.* **2009**, *13*, 124.
(29) Guo, Z.; Xing, R.; Liu, S.; Zhong, Z.; Ji, X.; Wang, L. Antifungal properties of Schiff bases of chitosan, N-substituted chitosan and quaternized chitosan. *Carbohydr. Res.* **2007**, *342*, 1329−1332.
(30) Wang, L.; Zheng, Z.; Yu, Z.; Zheng, J.; Fang, M.; Wu, J.; Tian, Y.; Zhou, H. Schiff Base Particles with Aggregation-Induced Enhanced Emission: Random Aggregation Preventing $\pi-\pi$ Stacking. *J. Mater. Chem. C* **2013**, *1*, 6952−6959.
(31) Zang, L.; Wei, D.; Wang, S.; Jiang, S. A Phenolic Schiff Base for Highly Selective Sensing of Fluoride and Cyanide via Different Channels. *Tetrahedron* **2012**, *68*, 636−641.
(32) Gupta, A. K.; Dhir, A.; Pradeep, C. P. A Fluorescence 'turn-on' Chemodosimeter for Selective Detection of Nb^{5+} Ions in Mixed Aqueous Media. *Dalton Trans.* **2013**, *42*, 12819−12823.
(33) Adams, M. J.; Highfield, J. G.; Kirkbright, G. F. Determination of Absolute Fluorescence Quantum Efficiency of Quinine Bisulfate in Aqueous Medium by Optoacoustic Spectrometry. *Anal. Chem.* **1977**, *49*, 1850−1852.
(34) Frisch, M. J.; Trucks, G. W.; Schlegel, H. B.; Scuseria, G. E.; Robb, M. A.; Cheeseman, J. R.; Scalmani, G.; Barone, V.; Mennucci, B.; Petersson, G. A.; Nakatsuji, H.; Caricato, M.; Li, X.; Hratchian, H. P.; Izmaylov, A. F.; Bloino, J.; Zheng, G.; Sonnenberg, J. L.; Hada, M.; Ehara, M.; Toyota, K.; Fukuda, R.; Hasegawa, J.; Ishida, M.; Nakajima, T.; Honda, Y.; Kitao, O.; Nakai, H.; Vreven, T.; Montgomery, J. A., Jr.; Peralta, J. E.; Ogliaro, F.; Bearpark, M.; Heyd, J. J.; Brothers, E.; Kudin, K. N.; Staroverov, V. N.; Kobayashi, R.; Normand, J.; Raghavachari, K.; Rendell, A.; Burant, J. C.; Iyengar, S. S.; Tomasi, J.; Cossi, M.; Rega, N.; Millam, J. M.; Klene, M.; Knox, J. E.; Cross, J. B.; Bakken, V.; Adamo, C.; Jaramillo, J.; Gomperts, R.; Stratmann, R. E.; Yazyev, O.; Austin, A. J.; Cammi, R.; Pomelli, C.; Ochterski, J. W.; Martin, R. L.; Morokuma, K.; Zakrzewski, V. G.; Voth, G. A.; Salvador, P.; Dannenberg, J. J.; Dapprich, S.; Daniels, A. D.; Farkas, O.; Foresman, J. B.; Ortiz, J. V.; Cioslowski, J.; Fox, D. J. *Gaussian 09*, revision B.01; Gaussian, Inc.: Wallingford, CT, 2010.
(35) Becke, A. D. Density-Functional Thermochemistry. III. The Role of Exact Exchange. *J. Chem. Phys.* **1993**, *98*, 5648−5652.
(36) Becke, A. D. Density-Functional Exchange-Energy Approximation with Correct Asymptotic Behavior. *Phys. Rev. A* **1998**, *38*, 3098−3100.
(37) Lee, C.; Yang, W.; Parr, R. G. Development of the Colle-Salvetti Correlation-Energy Formula into a Functional of the Electron Density. *Phys. Rev. B* **1998**, *37*, 785−789.
(38) Dreuw, A.; Head-Gordon, M. Single-Reference ab Initio Methods for the Calculation of Excited States of Large Molecules. *Chem. Rev.* **2005**, *105*, 4009−4037.
(39) Cossi, M.; Barone, V.; Cammi, R.; Tomasi, J. Ab Initio Study of Solvated Molecules: A New Implementation of the Polarizable Continuum Model. *Chem. Phys. Lett.* **1996**, *255*, 327−335.
(40) Pastore, M.; Mosconi, E.; Angelis, F.; Grätzel, M. A Computational Investigation of Organic Dyes for Dye-Sensitized Solar Cells: Benchmark, Strategies, and Open Issues. *J. Phys. Chem. C* **2010**, *114*, 7205−7212.
(41) Hankache, J.; Wenger, O. S. Photoinduced Electron Transfer in Covalent Ruthenium− Anthraquinone Dyads: Relative Importance of Driving-Force, Solvent Polarity, and Donor−Bridge Energy Gap. *Phys. Chem. Chem. Phys.* **2012**, *14*, 2685−2692.
(42) Hirota, J.; Okura, I. Photoinduced Intramolecular Electron Transfer in Bisviologen-Linked Porphyrin in Acetonitrile. *J. Phys. Chem.* **1993**, *97*, 6867−6870.
(43) Zhang, X.; Wang, J. Morpholine-Phthalocyanine (Donor−Acceptor) Construct: Photoinduced Intramolecular Electron Transfer

and Triplet Formation from its Charge Separation State. *J. Phys. Chem. A* **2011**, *115*, 8597−8603.
(44) Liu, X.; Iu, K. K.; Thomas, J. K. Photophysical Properties of Pyrene in Zeolites. Observation of Pyrene Anion Radicals in Zeolites X and Y. *Chem. Phys. Lett.* **1993**, *204*, 163−167.
(45) Rameshkumar, A.; Sivasudha, T.; Jeyadevi, R.; Sangeetha, B.; Arul Ananth, D.; Smilin Bell Aseervatham, G.; Nagarajan, N.; Renganathan, R.; Kathiravan, A. In Vitro Antioxidant and Antimicrobial Activities of Merremia Emarginata using Thio Glycolic Acid-capped Cadmium Telluride Quantum Dots. *Colloids Surf., B* **2013**, *101*, 74.
(46) Wu, X.; Li, H.; Liang, J.; Cheng, Y.; Hanu, H.; Liu, J.; Haley, K. N.; Treadway, J. A.; Larson, J. P.; Ge, N.; et al. Corrigendum: Immunofluorescent Labeling of Cancer Marker Her2 and other Cellular Targets with Semiconductor Quantum Dots. *Nature* **2003**, *21*, 41−46.
(47) Nagarajan, N.; Vanitha, G.; Arul Ananth, D.; Rameshkumar, A.; T. Sivasudha, T.; Renganathan, R. Bioimaging, Antibacterial and Antifungal properties of Imidazole-Pyridine Fluorophores: Synthesis, Characterization and Solvatochromism. *J. Photochem. Photobiol., B* **2013**, *127*, 212−222.
(48) Kashyap, D. R.; Wang, M.; Liu, L. H.; Boons, G. J.; Gupta, D.; Dziarski, R. Peptidoglycan Recognition Proteins Kill Bacteria by Activating Protein-Sensing Two-Component Systems. *Nature* **2011**, *17*, 676−683.
(49) Diao, W. R.; Hu, Q. P.; Zhang, H.; Xu, J. G. Chemical Composition, Antibacterial Activity and Mechanism of Action of Essential Oil from Seeds of Fennel (*Foeniculam vulgare Mill*). *Food Control* **2014**, *35*, 109.